

Density Matrix Reconstruction with Spin-polarized Current

Fabrício M. Souza*

Instituto de Física, Universidade Federal de Uberlândia, 38400-902 Uberlândia, MG, Brazil

(Dated: February 5, 2022)

We simulate a feasible experimental scenario that reconstruct the density matrix of an electronic qubit via spin-polarized tunneling currents. Our system is composed of a single level quantum dot, attached to ferromagnetic leads. By properly rotating the leads magnetizations we can select the spin component to be detected. Counting the number of tunneling events taken in four different magnetic alignments we find the Stokes parameters, that are used as a train data set into a supervised machine learning algorithm. The predicted model allows the complete knowledge of the open system density matrix, including both probability amplitudes and relative phases.

PACS numbers: 03.65.Yz, 73.23.-b, 03.67.-a

Keywords: open quantum systems & decoherence, quantum transport, quantum information with solid state qubits, machine learning.

Since the seminal work of Loss and DiVincenzo on quantum computation with single spins in quantum dots,[1] a wealth of experimental and theoretical studies on quantum information processing with quantum bits (qubit) based on the electron spin have arisen in the literature,[2] mainly motivated by the long spin decoherence times for electrons in semiconductors, and the ability to measure and control quantum-dot spins.[3] A few examples encompass the implementation of CNOT gates in semiconductor quantum dots using electron spin qubits,[4] \sqrt{SWAP} two-qubit exchange gate between electron spin qubits,[5] and both CZ and CNOT gates in double quantum dot structure.[6] Recently, it was shown a valley-orbit hybridization mechanism that protects electronic qubits in quantum dots from the effects of charge noise.[7]

The qubit state reconstruction is of fundamental importance for quantum technologies, as their characterization allows the study of properties such as probabilities of possible measurable outcomes, coherences and entanglement.[8] The field of quantum state tomography emerged in the context of quantum optics, with the development of tomography to reconstruct photonic states.[9–12]

In the context of electron spin, optical tomography schemes have also been successfully applied to characterize single electron spin states. For instance, time-resolved Kerr rotation spectroscopy allows a non-destructive observation of the spin precession in a quantum dot.[13] Tomographic Kerr rotation techniques have been developed to observe spin states of optically injected electrons in a semiconductor quantum well.[14] Also, tomographic methods have been applied to two and three-partite electronic systems.[15, 16] Additionally, via shot-noise, Jullien *et al.* reconstructed the wavefunction of single electrons in ballistic conductors, by repeatedly applying Lorentzian voltage pulses that injects on-demand electrons into a conductor.[17] Recently, Bisognin *et al.*

show fermionic quantum state reconstruction from electrical currents, thus opening the possibilities of quantum transport based tomography.[18]

The present work arises in this context as a theoretical proposal to reconstruct the density matrix of single electron spin qubit using spin-polarized quantum transport. Our system consists of a well known spintronic device based on a quantum dot attached to ferromagnetic leads.[19] The idea here is to probe spin-polarized tunneling processes that provide the probability distributions in different spin-quantization axes. With a sequence of identical initializations and subsequent tunneling detections, it becomes possible to reconstruct the entire density matrix of a single qubit. The main idea here encompasses the following steps: (1) a numerical calculation of the dynamics of a quantum dot attached to leads, that provides tunneling probability distributions as input of (2) an experimental scenario simulation (data acquisition) that uses stochastically generated data. From the collected counting data we determine (3) the Stokes parameters, that are used as a training set for (4) a supervised machine learning algorithm. With the predicted model we (5) reconstruct the whole quantum state, including probability amplitudes and relative phases.

Consider a closed single qubit model, with density matrix given by $\rho_0 = \frac{1}{2} \sum_{i=0}^3 S_i \sigma_i$, where σ_i are the Pauli matrices and S_i are the Stokes parameters, given by $S_i = \text{Tr}\{\sigma_i \rho_0\}$. The index 0 in the density matrix means closed system. Here, $S_0 = 1$ and $\sigma_0 = I$, where I is a 2×2 identity matrix. Each Stokes parameter corresponds to the outcome of projective measurements, taken along x , y or z direction, which is a well known technique to probe photonic qubits.[20] Here we propose to apply the same technique to probe the electronic qubit in quantum dots. To this aim we simulate an experimental scenario based on stochastic tunneling events between the quantum dot and drain leads.

We consider an open system composed of a quantum dot attached to ferromagnetic leads full polarized with their magnetization taken along some specific direction given by λ_s . This coupling is described in our model by

* fmsouza@ufu.br

the tunneling Hamiltonian[21]

$$H_T^{(\lambda,s)} = V \sum_k (c_{k,\lambda_s}^\dagger d_{\lambda_s} + h.c.), \quad (1)$$

where c_{k,λ_s}^\dagger creates one electron with wave vector k and spin λ_s in the drain. The operator d_{λ_s} annihilates one electron in the dot with spin λ_s . The parameter V gives the tunnel matrix element between the dot and the lead states. We assume V being independent of both the electron spin and energy (wideband limit). The quantum dynamics for the open system is governed by the von Neumann equation, $\dot{\rho}_{\text{tot}}(t) = -i[H, \rho_{\text{tot}}(t)]$ ($\hbar = 1$), with ρ_{tot} being the total density matrix defined in the space $\mathcal{E}_D \otimes \mathcal{E}_{\lambda_s}$, where \mathcal{E}_D and \mathcal{E}_{λ_s} stand for dot and leads subspaces, respectively. More than one lead can be attached to the dot, so we can have, for instance, $\mathcal{E}_{\lambda_+} \otimes \mathcal{E}_{\lambda_-}$ as leads subspace. The total Hamiltonian includes dot and leads Hamiltonians (free electron terms), as well as hopping terms. To find the reduced density matrix $\rho(t)$, which considers only quantum dot degrees of freedom, we take the partial trace related to the leads degree of freedom, i.e., $\rho(t) = \text{Tr}_{\text{lead}}\{\rho_{\text{tot}}(t)\}$, so we can write $\rho(t) = \sum_{i,j,l,m=0}^1 \rho_{ij,lm}(t) |ij\rangle \langle lm|$, where the complete computational basis reads $\{|00\rangle, |01\rangle, |10\rangle, |11\rangle\}$. Here $\rho_{00,00}$ gives a double occupancy probability, $\rho_{01,01} = \rho_{\uparrow\uparrow}$ and $\rho_{10,10} = \rho_{\downarrow\downarrow}$ provide the occupation probability for a single electron with spin $|\uparrow\rangle$ and $|\downarrow\rangle$, respectively, taken along z direction, and $\rho_{11,11}$ gives the zero occupancy probability. Double occupancy will not be accounted for in our model, as we assume that a single electron will be initialized in the quantum dot, and subsequently drained into one of the leads, i.e., the charge flows unidirectionally from dot to lead. This single occupancy can be achieved in the Coulomb blockade regime.[22]

Following Ref.[23], the relations between the Stokes parameters and probabilities p_{λ_s} of tunneling events for a specific spin orientation are written as

$$S_0 = 2p_0/(\delta\Gamma_0), \quad (2)$$

$$S_1 = 2(p_{x+} - p_0)/(\delta\Gamma_0), \quad (3)$$

$$S_2 = 2(p_{y+} - p_0)/(\delta\Gamma_0), \quad (4)$$

$$S_3 = 2(p_{z+} - p_0)/(\delta\Gamma_0), \quad (5)$$

where Γ_0 is a tunneling rate and δ a short enough time interval. Also $p_0 = (p_{z+} + p_{z-})/2$. The probability that a tunneling event occurs around time t_i in the λ_s polarized lead is given by

$$p_{\lambda_s}(t_i) = \Gamma_0 \int_{t_i - \delta/2}^{t_i + \delta/2} \langle \lambda_s | \rho(t_i + \tau) | \lambda_s \rangle d\tau. \quad (6)$$

If δ is small enough, we approximate $p_{\lambda_s}(t_i) \approx \delta\Gamma_0 \langle \lambda_s | \rho(t_i) | \lambda_s \rangle$, so we take

$$\begin{aligned} p_{x+} &= \delta\Gamma_0 \langle x+ | \rho | x+ \rangle \\ p_{y+} &= \delta\Gamma_0 \langle y+ | \rho | y+ \rangle \\ p_{z+} &= \delta\Gamma_0 \langle + | \rho | + \rangle. \end{aligned} \quad (7)$$

Here we use the notation $|\uparrow\rangle = |+\rangle$ and $|\downarrow\rangle = |-\rangle$ for spins taken along z direction. Rotating the basis, the $x+$ and $y+$ probabilities can be expressed as

$$\begin{aligned} p_{x+} &= \frac{\delta\Gamma_0}{2} (\langle + | \rho | + \rangle + \langle + | \rho | - \rangle + \langle - | \rho | + \rangle + \langle - | \rho | - \rangle) \\ p_{y+} &= \frac{\delta\Gamma_0}{2} (\langle + | \rho | + \rangle + i \langle + | \rho | - \rangle - i \langle - | \rho | + \rangle + \langle - | \rho | - \rangle). \end{aligned}$$

Additionally, $p_0 = \delta\Gamma_0 (\langle + | \rho | + \rangle + \langle - | \rho | - \rangle)/2$.

At this point we describe a stochastic approach used to simulate actual experimental conditions for the characterization of the qubit, where tunneling events are repeatedly counted. From the experimental point of view, to find p_{λ_s} we need to initialize and read-out R times the quantum system. For instance, one can photoexcite the quantum dot with circular polarized laser pulse, thus creating a single electron with spin up in the dot.[24],[25] This electron will eventually be drained into the lead after some time. This tunneling event can be detected with nowadays technologies.[26] For our simulations, we assume that the system is observed for some time interval T . We divide T in M smaller intervals of size δ , so that $T = M\delta$. If we repeat the experiment R times, with R being large enough, the probability p_{λ_s} will tend to $p_i = n_i/R$, where n_i is the number of times a particle was detected around i -th time interval in lead λ_s polarized.

We now proceed to determine the probability distributions behind the stochastic tunneling processes. Consider a set \mathcal{S} of integer numbers ranging from 1 to L , with $L \gg M$. We partitionate this set in $M+1$ subsets such that $s_1 \cup s_2 \cup \dots \cup s_M \cup s_{M+1} = \mathcal{S}$ and $s_i \cap s_j = \emptyset$ for $i \neq j$. If we say that subset s_i contains \mathcal{N}_i elements, we define

$$\frac{\mathcal{N}_1}{L} + \frac{\mathcal{N}_2}{L} + \dots + \frac{\mathcal{N}_M}{L} = \Gamma_{\lambda_s} \int_0^T \langle \lambda_s | \rho(t) | \lambda_s \rangle dt, \quad (8)$$

so that the sum $\mathcal{N}_1 + \mathcal{N}_2 + \dots + \mathcal{N}_M = Lf$, with f being a fraction of L , with the remainder inside the last subset s_{M+1} , i.e., $\mathcal{N}_{M+1} = L(1-f)$. Here the probability to detect a tunneling event at i -th time is given by $p_i = \mathcal{N}_i/L$. In the numerical implementation we follow a uniform distribution for the random selection of one element x in \mathcal{S} , if $x \in s_i$ ($i \leq M$) it means that a tunneling event was detected at the i -th time interval. Now we fix the \mathcal{N}_i distribution in such a way that expectation values make sense, i.e., we take $\mathcal{N}(s_i) = \text{int}(L\Gamma_0\delta \langle \lambda_s | \rho(t_i) | \lambda_s \rangle)$, where int means integer-valued function. We have to numerically find $\rho(t_i)$ and use it as an input to determine the distribution $\mathcal{N}(s_i)$.

The quantum dynamics of the open system is given in the standard Born-Markov approximation, via the Lindblad equation [27]

$$\dot{\rho} = -i[H_0, \rho] + \mathcal{L}_{\lambda_s}\rho, \quad (9)$$

where the superoperator \mathcal{L}_{λ_s} stands for tunneling processes. More specifically we write

$$\mathcal{L}_{\lambda_s}\rho = L_{\lambda_s}\rho L_{\lambda_s}^\dagger - \frac{1}{2}L_{\lambda_s}^\dagger L_{\lambda_s}\rho - \frac{1}{2}\rho L_{\lambda_s}^\dagger L_{\lambda_s}, \quad (10)$$

where $L_{\lambda_s} = \sqrt{\Gamma_0} d_{\lambda_s}$. The dot Hamiltonian is given by $H_0 = (\Omega/2) \sum_{\sigma,\sigma'} \hat{\mathbf{n}} \cdot \boldsymbol{\sigma}_{\sigma\sigma'} d_{\sigma}^{\dagger} d_{\sigma}$. Here $\hat{\mathbf{n}}$ specifies some magnetic field direction and Ω is a characteristic constant, proportional to the magnetic field strength. So this model allows a coherent spin dynamics in the dot, that will be probed by the tunneling events into ferromagnetic drains.

Figure (1) shows the tunneling events counted in each lead with one of the four spin polarizations, $|+\rangle$, $|-\rangle$, $|x+\rangle$ and $|y+\rangle$. We observe that the counting events present a damped oscillatory pattern along $+$, $-$ and $y+$ spin orientations. This is a result of the spin precession taken in the yz plane in the Bloch sphere, as we assume a transverse magnetic field taken along x direction. In particular, $+$ and $-$ components follow a damped Rabi like oscillations. In contrast, the counted events in $x+$ direction presents a monotonic exponential decay, as the spin projection in $x+$ direction does not oscillate in time. With the number of tunneling processes n_i found in Fig. (1), we determine p_i for each one of the four spin components considered. Using these probabilities in Eqs. (2)-(5) we determine the Stokes parameters $S_l(t_i)$ illustrated in Fig. (2). The parameter S_0 shows a simple exponential decaying, thus reflecting the decoherence imposed by the ferromagnetic leads. It is valid to note that from S_0 we can directly extract the tunneling rate. In contrast, S_1 presents a dispersion with mean value close to zero. This shows that both spin components $x+$ and $x-$ have equally probability amplitudes to tunnel out the dot. Finally, S_2 and S_3 present well defined damped oscillatory patterns, which reflects the dynamics taken in the yz plane.

In order to reconstruct the reduced density matrix, we apply a supervised machine learning algorithm.[28] The Stokes parameters $S_l(t_i)$ found in Fig. (2) are used as a set of train data, whose machine learning model interpolates. To this aim we construct $(d+1)$ -dimensional feature vectors of the form, $|\mathbf{t}_i\rangle = (1 \ t_i \ \dots \ t_i^{d-1} \ t_i^d)^T \in \mathbb{R}^{d+1}$, with $i = 1, \dots, M$. The estimators are obtained via linear regression model, $|\mathbf{b}_i^{(l)}\rangle = (b_{i0}^{(l)} \ b_{i1}^{(l)} \ \dots \ b_{i(d-1)}^{(l)} \ s_{id}^{(l)})^T$, which provides the predicted Stokes parameters $\hat{S}_l(t_i) = \langle \mathbf{b}_i^{(l)} | \mathbf{t}_i \rangle$, that minimize the cost function $j_l = \sum_i [S_l(t_i) - \hat{S}_l(t_i)]^2$ for each l . [29] The dimension $d+1$ should be properly adjusted depending on l in order to avoid both underfitting and overfitting problems. The solid black lines in Fig. (2) is the resulted $\hat{S}_l(t)$ model, that captures the main features of the randomly generated data $S_l(t_i)$.

Finally, in Fig. (3) we plug the obtained Stokes parameters model $\hat{S}_l(t)$ in $\hat{\rho} = \frac{1}{2} \sum_{l=0}^3 \hat{S}_l \sigma_l$. In panels (a) and (b) we show the diagonal elements $\hat{\rho}_{00} = \langle 0 | \hat{\rho} | 0 \rangle$ and

$\hat{\rho}_{11} = \langle 1 | \hat{\rho} | 1 \rangle$, respectively. As the system is initialized in $|0\rangle$ (spin up), we have $\hat{\rho}_{00}$ starting close to one. As time evolves both $\hat{\rho}_{00}$ and $\hat{\rho}_{11}$ present damped Rabi oscillations due to the presence of the transversal magnetic field. The dotted lines give the corresponding density matrix elements of the closed system, i.e., without leads. In

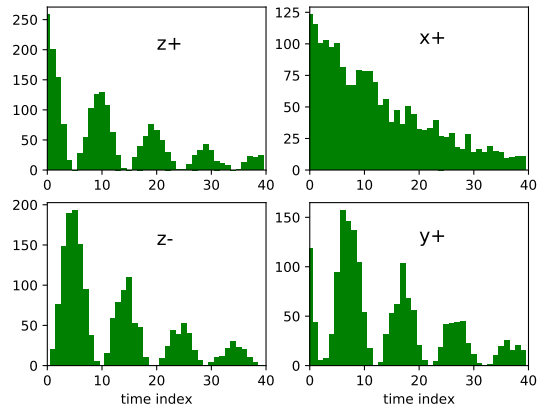


FIG. 1. Count of tunneling events as function of time for spin orientations along (a) $z+$, (b) $z-$, (c) $x+$ and (d) $y+$. The $z+$ component starts with high counting number due to the initialization state $|\uparrow\rangle$. As time evolves, both $z+$ and $z-$ present bunches of tunneling events, reflecting the characteristic Rabi oscillations taken place in a two level system. The bunches vanish as time evolves due to the decoherence process imposed by the drain leads. The $y+$ component also presents an oscillatory damped pattern, while the $x+$ counted tunneling events show just an exponential decaying rate.

panels (c) and (d) we show the real and imaginary parts of $\langle 0 | \hat{\rho} | 1 \rangle$, respectively. While the real part presents no dynamics, the imaginary part oscillates, tending to zero as time evolves. Note that with increasing time the off-diagonal element of $\hat{\rho}$ vanishes due to decoherences. Also, both $\hat{\rho}_{00}$ and $\hat{\rho}_{11}$ vanish as the charge is being drained to the leads.

In conclusion, we have simulated an experimental scenario of spin-polarized charge tunneling detection in a quantum dot system attached to ferromagnetic leads, that allows the full reconstruction of quantum state dynamics. By counting the number of tunneling events in four different spin orientations we obtain the Stokes parameters, that are used as train data set in a supervised machine learning algorithm that predicts the entire behavior of the Stokes parameters. This allows to reconstruct the density matrix of the system, including both probability amplitudes and relative phases.

Data Availability Statement. The data that supports the findings of this study are available from the corresponding author upon reasonable request.

[1] D. Loss and D. P. DiVincenzo, Phys. Rev. A **57**, 120 (1998).

[2] X. Zhang, H.-O. Li, G. Cao, M. Xiao, G.-C. Guo, and

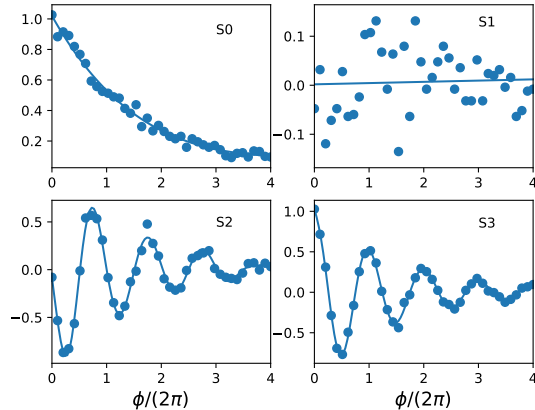


FIG. 2. Simulation of data acquisition for Stokes parameters. Using the counting statistics found in Fig. (1) we determine the probability p_i to detect tunneling events for each one of the four spin directions $+$, $-$, $x+$ and $y+$. From that the Stokes parameters $S_i(t_i)$ are found. The solid lines show the machine learning model $\hat{S}_i(t)$ obtained for the Stokes parameters. Parameters: $\phi = \Omega t$ and $\Gamma_0 = 0.1\Omega$.

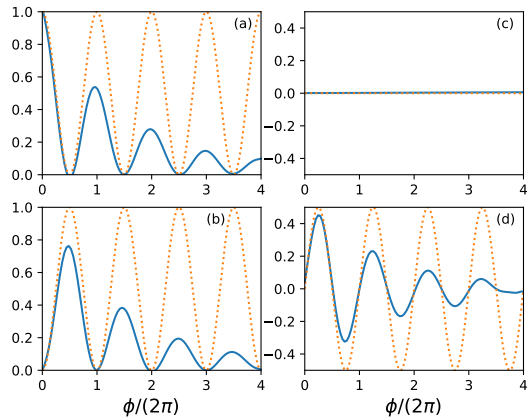


FIG. 3. Reconstructed density matrix. The solid lines show the density matrix obtained from the machine learning model for $\hat{S}_i(t)$, that is plugged in $\hat{\rho}(t) = (1/2)\sum_i \hat{S}_i(t)\sigma_i$. In panels (a) and (b) we show the diagonal elements $\langle 0|\hat{\rho}|0\rangle$ and $\langle 1|\hat{\rho}|1\rangle$, that shows characteristic damped Rabi oscillations. The dotted lines show the analytical theoretical density matrix derived for a closed system. In panels (c) and (d) we show, respectively, real and imaginary parts of $\langle 0|\hat{\rho}|1\rangle$. So the entire density matrix is recovered, which means that we have the full information of the quantum state, i.e., both probability amplitudes and relative phase. Parameters: $\phi = \Omega t$ and $\Gamma_0 = 0.1\Omega$.

G.-P. Guo, Nat. Sci. Rev. **6**, 32 (2018).

- [3] J. Yoneda, K. Takeda, T. Otsuka, T. Nakajima, M. R. Delbecq, G. Allison, T. Honda, T. Kodera, S. Oda, Y. Hoshi et al., Nat. Nanotechnol. **13**, 102 (2018).
- [4] D. M. Zajac, A. J. Sigillito, M. Russ, F. Borjans, J. M. Taylor, G. Burkard, and J. R. Petta, Science **359**, 439 (2018).
- [5] Y. He, S. K. Gorman, D. Keith, L. Kranz, J. G. Keizer, and M. Y. Simmons, Nature (London) **571**, 371 (2019).
- [6] M. Russ, D. M. Zajac, A. J. Sigillito, F. Borjans, J. M. Taylor, J. R. Petta, and G. Burkard, Phys. Rev. B **97**, 085421 (2018).
- [7] X. Mi, S. Kohler, and J. R. Petta, Phys. Rev. B **98**, 161404(R) (2018).
- [8] M. Cramer, M. B. Plenio, S. T. Flammia, R. Somma, D. Gross, S. D. Bartlett, O. L.-Cardinal, D. Poulin, and Y.-K. Liu, Nat. Commun. **1**, 149 (2010).
- [9] K. Vogel and H. Risken, Phys. Rev. A **40**, 2847(R) (1989).
- [10] D. T. Smithey, M. Beck, M. G. Raymer, and A. Faridani, Phys. Rev. Lett. **70**, 1244 (1993).
- [11] G. M. D'Ariano, U. Leonhardt, and H. Paul, Phys. Rev. A **52**, R1801 (1995).
- [12] S. Schiller, G. Breitenbach, S. F. Pereira, T. Müller, and J. Mlynek Phys. Rev. Lett. **77**, 2933 (1996).
- [13] M. H. Mikkelsen, J. Berezovsky, N. G. Stoltz, L. A. Coldren, and D. D. Awschalom, Nature Physics **3**, 770 (2007).
- [14] H. Kosaka, T. Inagaki, Y. Rikitake, H. Imamura, Y. Mitsumori, and K. Edamatsu, Nature **457**, 702 (2009).
- [15] J. Medford, J. Beil, J. M. Taylor, S. D. Bartlett, A. C. Doherty, E. I. Rashba, D. P. DiVincenzo, H. Lu, A. C. Gossard, and C. M. Marcus, Nature Nanotechnology **8**, 654 (2013).
- [16] M. D. Shulman, O. E. Dial, S. P. Harvey, H. Bluhm, V. Umansky, A. Yacoby, Science **336**, 202 (2012).
- [17] T. Jullien, P. Roulleau, B. Roche, A. Cavanna, Y. Jin,

and D. C. Glatli Nature **514**, 603 (2014).

- [18] R. Bisognin, A. Marguerite, B. Roussel, M. Kumar, C. Cabart, C. Chapelaine, A. Mohammad-Djafari, J.-M. Berroir, E. Bocquillon, B. Plaçais, A. Cavanna, U. Gennser, Y. Jin, P. Degiovanni, and G. Fève, Nature Communications **10**, 3379 (2019).
- [19] F. M. Souza, Phys. Rev. B **76**, 205315 (2007).
- [20] J. B. Altepeter, D. F. V. James, and P. G. Kwiat, Qubit Quantum State Tomography, Lect. Notes Phys. **649**, 113 (2004).
- [21] S. Weiss and J. König, Phys. Rev B **96**, 064529 (2017).
- [22] *Single Charge Tunneling: Coulomb Blockade Phenomena in Nanostructures*, Eds. H. Grabert and M. H. Devoret, NATO ASI Series B: Physics **294**, Plenum, New York (1992).
- [23] D. F. V. James, P. G. Kwiat, W. J. Munro, and A. G. White, Phys. Rev. A **64**, 052312 (2001).
- [24] T. Fujita, K. Morimoto, H. Kiyama, G. Allison, M. Larson, A. Ludwig, S. R. Valentin, A. D. Wieck, A. Oiwa, and S. Tarucha, arXiv:1504.03696.
- [25] J. M. Villas-Bôas, S. E. Ulloa, and A. O. Govorov, Phys. Rev. B **75**, 155334 (2007).
- [26] A. Kurzman, P. Stegmann, J. Kerski, R. Schott, A. Ludwig, A. D. Wieck, J. König, A. Lorke, and M. Geller, Phys. Rev. Lett. **122**, 247403 (2019).
- [27] G. Lindblad, Commun. Math. Phys. **48**, 119 (1976).
- [28] F. Pedregosa, G. Varoquaux, A. Gramfort, V. Michel, B. Thirion, O. Grisel, M. Blondel, P. Prettenhofer, R. Weiss, V. Dubourg, J. Vanderplas, A. Passos, D. Cournapeau, M. Brucher, M. Perrot, E. Duchesnay, J. Mach. Learn. Res. **12**, 2825 (2011).
- [29] P. Wilmott, *Machine Learning: An Applied Mathematics*

Introduction, 1st ed. (Panda Ohana Publishing, 2019).